

Characterization of two novel ammonia transporters, Hiat1a and Hiat1b, in the teleost model system *Danio rerio*

Haonan Zhouyao¹, Alex M. Zimmer^{2,3}, Sandra Fehsenfeld⁴, Thomas Liebenstein⁵, David O. Richter⁵, Gerrit Begemann⁵, Peter Eck¹, Steve F. Perry³, Dirk Weihrauch^{6,*}

¹University of Manitoba, Department of Food and Human Nutritional Sciences, 66 Chancellors Circle, Winnipeg, MB - R3T 2N2, Canada

²University of Alberta, Department of Biological Science, 11355 Saskatchewan Drive, Edmonton, AB - T6G 2E9, Canada

³University of Ottawa, Department of Biology, 30 Marie Curie, Ottawa ON - K1N 6N5, Canada

⁴Université du Québec à Rimouski, Département de biologie, chimie et géographie, 300 Allée des Ursulines, Rimouski, QC - G5L 3A1, Canada

⁵Universität Bayreuth, Department of Biology, Universitätsstr. 30, University of Bayreuth, 95440 Bayreuth, Germany

⁶University of Manitoba, Department of Biological Sciences, 66 Chancellors Circle, Winnipeg, MB R3T 2N2, Canada

*Corresponding author: Dirk Weihrauch
University of Manitoba, Department of Biological Sciences, 66
Chancellors Circle
Winnipeg, MB - R3T 2N2, Canada
Email address: Dirk.Weihrauch@umanitoba.ca
Phone: 204-474-6310

Keywords: Morpholino, SIET, *In situ* hybridization, zebrafish larvae

Abstract

Ammonia excretion in fish excretory epithelia is a complex interplay of multiple membrane transport proteins and mechanisms. Using the model system of zebrafish (*Danio rerio*) larvae, here we identified three paralogues of a novel ammonia transporter, hippocampus abundant transcript 1 (DrHIAT1), found also in most vertebrates. When functionally expressed in *Xenopus laevis* oocytes, DrHiat1a and DrHiat1b promoted methylamine uptake in a competitive manner with ammonia. *In situ* hybridization experiments showed that both transporters were expressed as early as the 4-cell stage in zebrafish embryos and could be identified in most tissues four days post fertilization. Larvae experiencing morpholino-mediated knockdown of DrHiat1b exhibited significantly lower whole body ammonia excretion rates compared to control larvae. Markedly decreased site-specific total ammonia excretion of up to 85% was observed in both the pharyngeal region (site of developing gills) and the yolk sac (region shown to have the highest NH_4^+ flux). This study is the first to identify especially DrHiat1b as an important contributor to ammonia excretion in larval zebrafish. Being evolutionarily conserved, these proteins are likely involved in multiple other general ammonia-handling mechanisms, making them worthy candidates for future studies on nitrogen regulation in fishes and across the animal kingdom.

Introduction

Ammonia is a toxic waste product generated by the catabolism of proteins and nucleic acids, but also *via* ureolytic and uricolytic pathways (Larsen et al., 2014) (in the current study, NH_4^+ refers to the ammonium ion, NH_3 to gaseous ammonia, and ammonia to the sum of both). Ammonia is a weak base with a pK_a of 9.0 - 9.5 and occurs accordingly in physiological solutions dominantly (> 90%) in its ionic form, NH_4^+ , while only a small portion is present as the membrane permeable NH_3 (Cameron and Heisler, 1983). In fishes, elevated plasma ammonia levels caused by exercise or feeding (Bucking, 2017; Fehsenfeld and Wood, 2018; Sinha et al., 2012a; Sinha et al., 2012b) need to be tightly regulated to avoid negative physiological implications. Furthermore, when exposed to non-lethal high environmental ammonia (HEA), the resulting internal plasma ammonia load can cause a wide range of deleterious effects in fish, including disruption of general ion homeostasis (Diricx et al., 2013; Wilkie, 1997), reduced swimming performance (McKenzie et al., 2009; McKenzie et al., 2003; Shingles et al., 2001),

changes in energy metabolism (Arillo et al., 1981; Sinha et al., 2012a), and a reduced growth rate (Dosdat et al., 2003). To avoid its negative side effects, ammonia needs to be rapidly excreted from the body fluids. With a few exceptions, teleost fishes are ammoniotelic and excrete up to 90% of their metabolically produced ammonia directly through the gills (Sayer and Davenport, 1987; Smith et al., 2012; Smith, 1929; Zimmer et al., 2014).

In 2009, Wright and Wood published a working model for the branchial ammonia excretion mechanisms in a freshwater fish with the contribution of Rhesus-glycoproteins (Wright & Wood, 2009). It is assumed that plasma ammonia enters the epithelial cell in its gaseous form NH_3 via a basolateral localized Rhesus-glycoprotein, Rhbg, along its partial pressure gradient. Further, Mallery (1983) and Nawata et al. (2010) showed that similarly to invertebrates (Adlimoghaddam et al., 2015; Hans et al., 2018; Masui et al., 2002) and the mammalian kidney (Wall and Koger, 1994), teleost Na^+/K^+ -ATPase (NKA) is capable of accepting NH_4^+ instead of K^+ as a substrate. Consequently, in addition to NH_3 uptake via Rhbg, the basolateral NKA may mediate an active uptake of extracellular NH_4^+ into the branchial epithelial cell. The capacity of NKA to accept NH_4^+ as a substrate, however, seems to be dependent on external salinity and varies substantially among fishes (Wood and Nawata, 2011).

According to the model (Wright and Wood, 2009), it is further assumed that cytoplasmatic ammonia is excreted apically in a sodium-dependent manner via an apical $\text{Na}^+/\text{NH}_4^+$ exchange complex (Ito et al., 2013; Wright and Wood, 2009). This complex is thought to act as a metabolon that promotes the acidification of the unstirred boundary layer by means of a V-type H^+ -ATPase and Na^+/H^+ -exchanger 3, with both transporters creating a partial pressure gradient for gaseous NH_3 . NH_3 follows this gradient utilizing another Rhesus-glycoprotein, Rhcgb (formerly Rhcg1, Nakada et al., 2007), a process commonly referred as ammonia trapping. A membrane-bound carbonic anhydrase (CA2a and/or CA15a, Ito et al., 2013) supports this metabolon by catalyzing the hydration of CO_2 , providing the required H^+ for the process (Wright and Wood, 2009). A similar ammonia excretion mechanism has also been proposed for freshwater planarians (Weihrauch et al., 2012). An equivalent mechanism, i.e., sodium-dependent apical $\text{Na}^+/\text{NH}_4^+$ exchange metabolon, however, could not be verified for freshwater leeches, where the cutaneous ammonia excretion process was shown to be independent of functional apical Na^+ channels and NHEs (Quijada-Rodriguez et al., 2017). Furthermore, in the nematode *Caenorhabditis elegans*, knock-out of the apically localized Rh-protein RHR-2 caused a reduction in ammonia excretion rates; the remaining flux was, however, independent of environmental pH, in contrast to the wild-type (Adlimoghaddam et al., 2016). However, in

contrast to predictions stemming from the metabolon model (Wright and Wood, 2009), knocking out the apical Rhcgb in zebrafish *via* CRISPR/Cas9 did not reduce ammonia excretion and/or Na^+ -uptake. Rather, an increase in ammonia excretion was observed (Zimmer and Perry, 2020). The diversity of ammonia excretory mechanisms across fishes and other aquatic animals underlies their importance for nitrogen homeostasis, and at the same time warrants the consideration of additional routes and mechanisms.

In invertebrates, for example, NH_4^+ -transporting ammonium transporters (AMTs, also members of the AMT/MEP/Rh-protein ammonia transporter family) driven by the cytoplasm-to-environment electrochemical gradient of the cation, were suggested to be involved in the epithelial ammonia excretion process (clams: Boo et al., 2018; insects: Chasiotis et al., 2016; Durant and Donini, 2018; Pitts et al., 2014; polychaeta: Thiel et al., 2017). In vertebrates, however, AMTs have not been shown to be expressed to date.

An additional potential contributor to the branchial ammonia excretory process is the hippocampus-abundant transcript 1 (Hiat1). This presumptive ammonia transporter (CmHiat1) was associated with acid-base regulation in the green crab, *Carcinus maenas*, because its mRNA levels were decreased when the animals were acclimated to elevated P_{CO_2} levels (Fehsenfeld et al., 2011). Recently, it was demonstrated that CmHiat1 acts as an ammonia (likely NH_4^+) transporter in this species (Fehsenfeld et al., 2022 under review) with its mRNA abundance found up-regulated in response to high environmental ammonia.

In light of the results of these studies, the current study was designed to test the hypothesis that Hiat1 is involved in ammonia excretion in zebrafish larvae. To address these hypotheses, we investigated Hiat1 function using multiple physiological and molecular techniques. After identifying and characterizing Hiat1 paralogues in a phylogenetic analysis, we expressed DrHiat1a and DrHiat1b proteins in frog oocytes to verify their capability of transporting methylamine (ammonia analog) competitively with NH_4Cl . We then determined mRNA expression patterns of both paralogs throughout early development (4-cell stage to 4 days post fertilization) by *in situ* hybridization. Lastly, we knocked down DrHiat1a and DrHiat1b using morpholino injections and applied the scanning ion-selective electrode technique (SIET) to identify regions of interest of Hiat1-related ammonia flux in the *D. rerio* larvae in early development.

Material and methods

Sequence-based genetic structure analysis

DrHiat1-like (GenBank accession no. XP_002663499.2; 500 aa), DrHiat1b (GenBank accession no. AAH97075.1, 485 aa), and the translated DrHiat1a protein based on the open reading frame (ORF) of zebrafish *DrHiat1a* (GenBank accession no. BC056817, 493 aa) were aligned with Clustal Omega (<https://www.ebi.ac.uk/Tools/msa/clustalo/>). Protter (Omasits et al., 2014) was used to predict transmembrane domains (TM) and the potential phosphorylation sites for all three Hiata1 proteins, and Scansite 4.0 (Obenauer et al., 2003) was used to identify the binding motifs. All transmembrane models and proteoform predictions were performed using the system's default settings.

DrHiat1b was then used to identify Hiata1 isoforms in other species *via* GenBank-BLASTp search (Table S1) (Altschul et al., 1997). Proteins were aligned with the MUSCLE algorithm as provided by the Molecular Evolutionary Genetics Analysis across computing platforms (MEGA X (Kumar et al., 2018)) using default settings. The evolutionary history was inferred by using the Maximum Likelihood method and JTT matrix-based model (Jones et al., 1992) as identified by the included testing function provided by MEGA X. Initial tree(s) for the heuristic search were obtained automatically by applying Neighbor-Join and BioNJ algorithms to a matrix of pairwise distances estimated using a JTT model, and then selecting the topology with superior log likelihood value. A discrete Gamma distribution was used to model evolutionary rate differences among sites (5 categories (+G, parameter = 0.3614)). All positions with less than 95% site coverage were eliminated, i.e., fewer than 5% alignment gaps, missing data, and ambiguous bases were allowed at any position (partial deletion option).

Heterologous expression of DrHiat1a and DrHiat1b in *Xenopus* oocytes

cDNA clones containing the full ORFs of *DrHiat1a* (clone ID: 2640969; GenBank accession number BC056817.1) and *DrHiat1b* (clone ID: 2600163, GenBank accession number BC097075) were purchased from Dharmacon (Lafayette, CO, USA). DNA miniprep kits (Qiagen, Hilden, Germany) were used to extract the plasmids following the manufacturer's guidance. Regular PCR employing Q5 High-Fidelity DNA Polymerase was used to obtain the full ORFs of *DrHiat1a* and *DrHiat1b* (see Table S2, ORF). The annealing temperature used for the amplification of *DrHiat1a* and *DrHiat1b* ORFs were 60°C and 62°C respectively with a total

of 35 cycles. Subsequently, regular PCR was used to add restriction enzyme sites to the 5' and 3' ends of the ORFs of *DrHiat1a* and *DrHiat1b* (see Table S2, oocytes). The annealing temperature used for the amplification of *DrHiat1a* and *DrHiat1b* ORFs were both 65°C with a total of 35 cycles. The quality of the DNA was assessed by gel electrophoresis and the concentration of DNA was determined spectrophotometrically after purification (GeneJET PCR purification kit, ThermoFisher, Waltham, MA, USA). The ORFs were then cloned into the pGEM®-HE plasmid, a modified pGEM®-3Z vector containing the *Xenopus* beta globin 5'- and 3'- UTR sequences using T4 ligase following the manufacturer's guidance (New England Biolabs (NEB), Ipswich, MA, USA). The *in vitro* transcription of capped mRNA (cRNA) was performed with HiScribe™ T7 ARCA mRNA kit (NEB) followed with column purification (RNeasy MinElute Cleanup Kit, Qiagen, Hilden, Germany). The cRNA was quantified spectrophotometrically (Nanodrop, ND-1000, Thermofisher, Waltham, MA, USA) and integrity was assessed on a MOPS agarose gel containing formaldehyde.

Stage VI-V oocytes were collected from mature female *Xenopus laevis* (VWR, Radnor, PA, USA) as previously described (Soreq and Seidman, 1992) (Protocol Reference# F20-021). Briefly, the frogs were euthanized *via* decapitation prior to the collection of the ovary. The ovary was placed in Ca²⁺-free OR2 (contained (in mmol l⁻¹) 82.5 NaCl, 2.5 KCl, 1 MgCl₂, 1 Na₂HPO₄, 5 HEPES, pH 7.2) solution with collagenase type VI (1 mg ml⁻¹) (Gibco, Waltham, MA, USA) and gently agitated for 90 minutes at room temperature. 1 mmol l⁻¹ CaCl₂ was added to terminate the collagenase activity. Oocytes were then manually sorted and rinsed three additional times with standard OR2 solution. For overnight storage of isolated oocytes, OR2 was supplemented with 2.5 mmol l⁻¹ sodium pyruvate, 1 mg mL⁻¹ penicillin-streptomycin (Gibco, Long Island, NY, USA) and 50 µg ml⁻¹ gentamicin at 16 °C. All procedures used were approved by the University of Manitoba Animal Research Ethics Board and are in accordance with the Guidelines of the Canadian Council on Animal Care.

Isolated oocytes after the overnight recovery were injected with 18.4 ng of cRNA (36.8 nl with 0.5 ng nl⁻¹) or nuclease-free water as control using the Nanoject II auto-nanoliter injector (Drummond Scientific, Broomall, PA, USA). Experiments were conducted 48 hours post-injection.

[H³] methylamine transport studies in oocytes expressing DrHiat1a and DrHiat1b

[H³] methylamine uptake experiments

Experiments were conducted at room temperature in 200 µl of standard OR2, pH 7.2, containing 3 µmol l⁻¹ (9.3 µCi) [H³]-methylamine (Moravek Inc., USA) with 60 minutes of incubation time. For each experiment 20 oocytes injected with either with cRNA or water (sham) were randomly selected. At the end of each experiment, ice-cold standard OR2 was used to terminate [H³] methylamine uptake by washing oocytes three times to remove the external radioactivity. The washed oocytes were immediately solubilized individually in 200 µl of 10% SDS (Sigma) to assess the internal radioactivity employing 5 ml of Ultima-Gold scintillation cocktail (PerkinElmer) and liquid scintillation counting (Tri-Carb 2900 TR; PerkinElmer). The effect of washing was determined by assessing the radioactivity in 200 µl standard OR2 used for the third washing post radioactive exposure compared to fresh, radioactivity-free standard OR2 at the same volume. For NH₄Cl competitive uptake experiments, the same procedures described above were conducted, however in the presence of 1 mmol l⁻¹ NH₄Cl added to the incubation solution.

[H³] methylamine release experiments

To determine whether Hiat proteins mediate bi-directional methylamine transport, the efflux of methylamine from SHAM oocytes, DrHiat1a-, and DrHiat1b-expressing oocytes were measured. Experiments were performed at room temperature in 200 µl of standard OR2 containing 3 µmol l⁻¹ (9.3 µCi) [H³] methylamine adjusted to pH 7.2 with 60 minutes of incubation time. Two groups of cRNA injected oocytes (n = 20) and two groups of water injected oocytes (n = 20) were assessed for each experimental point. Each group was considered as one replicate and overall, two replicates were done. After termination of [H³] methylamine uptake as described above, one group of cRNA injected oocytes and one group of water injected oocytes were immediately solubilized individually to assess the uptake of [H³] methylamine as described above, to determine the starting point for the following release experiment. The remaining groups of cRNA injected oocytes and water injected oocytes were placed in 200 µl of room temperature, radioactivity-free standard OR2 for 60 minutes for release and afterwards washed three times with ice-cold standard OR2, solubilized individually in 200 µl of 10% SDS and assess for remaining internal radioactivity. The efficiency of the washing steps was determined by

assessing 200 µl of the radioactivity of the third washing post radioactive exposure compared to fresh, radioactivity-free standard OR2 at the same volume.

***In situ* hybridization**

DrHiat1a and *DrHiat1b* ORFs were amplified and cloned as described above with Q5 High Fidelity DNA Polymerase (NEB) and primers located at both ends of the ORFs with restriction enzyme sites (Table S2, *in situ*).

The deletion of the *Xenopus* beta globin 5' UTR was done by removing a 63 bp fragment containing the 5' *Xenopus* UTR with KpnI and XmaI followed by blunting with Quick Blunting Kit (NEB) followed by re-ligation. The *Xenopus* beta globin 3' UTR was removed in the course of the linearization of the vector for the preparation of antisense-RNA probe. The antisense-RNA probe was synthesized as previously described (Thisse and Thisse, 2008) and experiments were conducted at the University of Bayreuth, Germany, using the Casper strain (White et al., 2008). Adult fish were maintained under standard conditions (14:10 h light:dark-cycle; 0.1 g l⁻¹ salinity; 300 µS conductivity; pH 7.5) at 27.5 - 28.5 °C. Embryos were obtained from pairing events of 3 male and 2 female fish and were reared in E3-medium (contained (in mmol l⁻¹) 5 NaCl, 0.17 KCl, 0.33 CaCl₂, 0.33 MgSO₄, 10-5% methylene blue; pH 7.2) at 28.5 °C.

Zebrafish embryos and larvae were euthanized on ice, fixed in 4 % PFA/PBS, washed in PBS/0,1 % Tween 20 (PBTw), transferred to 100 % methanol and stored at least overnight at -20 °C. After rehydration using a methanol/PBTw series and post-fixation in 4 % PFA/PBS, older developmental stages were treated with 10 µg ml⁻¹ proteinase K (Fermentas, Waltham, MA, USA) for 10 min (2 dpf), 15 min (3 dpf) and 20 min (4 dpf), respectively, post-fixed in 4% PFA/PBS and washed several times in PBTw. After hybridization with the corresponding antisense probes over night at 68 °C, the samples were washed in a formamide solution/PBTw series, blocked in 0.5 % blocking reagent, incubated in a 1:2000 dilution of anti-DIG-AP antibody in 0.5 % blocking reagent for 4 hours at room temperature and washed several times in PBTw. For detection, samples were equilibrated in BCL buffer and stained with NBT and BCIP/X-phos until staining was clearly visible.

Ammonia excretion studies in zebrafish with DrHiat1a or DrHiat1b knockdown

Zebrafish

Danio rerio originally purchased from the pet trade (Big Al's Aquarium, Ottawa, ON, Canada) were maintained in flow-through aquaria receiving dechlorinated city of Ottawa tap water ("system water"; in mmol l⁻¹: 0.8 Na⁺, 0.4 Cl⁻, 0.25 Ca²⁺; pH = 7.6) and held at 28.5 °C with a photoperiod of 14:10 hours light:dark. Embryos were obtained from breeding events between 1 male and 2 females held in static tanks. Embryos were reared in 60 ml Petri dishes containing system water with 0.05% methylene blue at a density of approximately 50 embryos per dish held at 28 °C. Handling and experimentation of zebrafish was conducted in compliance with the University of Ottawa Animal Care and Veterinary Service (ACVS) guidelines under protocol BL-1700 and followed the recommendations from the Canadian Council for Animal Care (CCAC).

Morpholino injections

Splice-blocking morpholino oligonucleotides (Gene Tools, LLC, Philomath, OR, USA) targeting the intron-exon junction between intron and exon 4 of *DrHiat1a* (NCBI accession: NM_199584.1; 5'-CATGGTGAGAGCCTCTGAAATCAAG-3'), targeting the intron-exon junction between intron and exon 4 of *DrHiat1b* (NCBI accession: NM_213527.2; 5'-AAAGTGAGGAGCGTAACGAACCATG-3'), and a standard control morpholino with no biological target in zebrafish (5'-CCTCTTACCTCAGTTACAATTTATA-3') were suspended to a final concentration of 2-4 ng morpholino nl⁻¹ in Danieau buffer (in mmol l⁻¹: 58 NaCl, 0.7 KCl, 0.4 MgSO₄, 0.6 Ca(NO₃)₂, and 5.0 HEPES buffer; pH 7.6) containing 0.05% phenol red for injection visualization. 1-cell stage embryos were injected with 1 nl of this injection solution [4 ng/embryo for DrHiat1a morpholino (MO), 4 ng/embryo for DrHiat1b MO, and 4 ng/embryo for control (sham) MO] using an IM 300 microinjection system (Narishige, Amityville, NY, USA). However, we observed a large proportion (>50%) of morphological abnormalities (curved tail/spine) with the 4 ng DrHiat1b dose and therefore used a dose of 2 ng for DrHiat1b and observed virtually no morphological abnormalities (<5-10%). Injections were verified at 1 dpf by examining the distribution of carboxyfluorescein (tagged to each morpholino) in individual embryos under a fluorescence dissecting microscope (Nikon SMZ1500, Nikon Instruments, Melville, NY, USA). Embryos that were successfully injected, containing a homogenous distribution of fluorescein signal, were reared as described above.

Knockdown was confirmed by reverse transcription PCR (RT-PCR). At 4 dpf, approximately 20 pooled larvae (n=1) from each treatment group (DrHiat1a MO, DrHiat1b MO, and sham MO) were euthanized by an overdose of neutralized tricaine methanesulfonate (MS-222; Syndel Canada, Nanaimo, BC, Canada), flash frozen in liquid nitrogen, and stored at -80 °C. RNA was extracted from pooled samples using Trizol (ThermoFisher, Waltham, MA, USA) following the manufacturer protocol. Extracted RNA was treated with DNase (ThermoFisher) and cDNA was then synthesized from 700 ng total RNA using the iScript cDNA synthesis kit (Bio-Rad, Hercules, CA, USA). RT-PCR was performed using DreamTaq DNA polymerase (ThermoFisher) following manufacturer's guidance and primers specific to DrHiat1a and DrHiat1b (see Table S2) The reaction volume for each PCR reaction was 20 µl with 55°C annealing temperature and the reaction was terminated after 40 cycles.

Whole-body ammonia flux

At 4 dpf, DrHiat1a, DrHiat1b, and sham MO-treated larvae were placed into 2 ml centrifuge tubes containing 1.5 mL system water (6 larvae/tube; n=1) maintained at 28-30 °C in a water bath. Larvae were allowed to adjust for 30 min where thereafter, initial 0.5 ml water samples were drawn from each tube, marking the beginning of the flux period. Following a 6-hours flux period, final 0.5 ml water samples were drawn from each tube. Samples were frozen and stored at -20 °C for no longer than 1 week. Total ammonia concentration (T_{Amm}) was measured using the indophenol method (Verdouw et al., 1978) and ammonia excretion rate ($\text{nmol larva}^{-1} \text{h}^{-1}$) was calculated using the following equation:

$$\text{Ammonia excretion} = [(T_{\text{Ammf}} - T_{\text{Ammi}}) * V] / t / n \quad (\text{Eqn 1})$$

where T_{Ammf} and T_{Ammi} (nmol ml^{-1}) are the final and initial total ammonia concentrations, respectively, V is volume (ml), t is flux duration (h), and n is the number of larvae in the tube.

Scanning Ion-selective micro-Electrode technique (SIET)

SIET was performed to assess NH_4^+ fluxes by 4 dpf larvae treated with sham and DrHiat1b morpholino. Measurements were made in a K^+ -free medium which was made by adding stock

solutions of Na_2SO_4 , CaCl_2 , $\text{MgSO}_4 \cdot 7\text{H}_2\text{O}$, Na_2HPO_4 , and NaH_2PO_4 to doubly distilled water (in mmol l^{-1} : 0.84 Na^+ , 0.5 Cl^- , 0.25 Ca^{2+} , 0.15 Mg^{2+} ; $\text{pH} = 7.6$). The omission of K^+ in the medium is necessary because this ion interferes with NH_4^+ signals from the ion-selective probe. In addition, the medium contained MS-222 anaesthetic (0.2 g l^{-1}) and $0.05 \text{ mmol l}^{-1} (\text{NH}_4)_2\text{SO}_4$, the latter being necessary because the Nernstian slope of the NH_4^+ tends to fall at concentrations below 0.1 mmol l^{-1} .

NH_4^+ -selective probes were constructed as described previously (Donini and O'Donnell, 2005). Glass capillary tubes (World Precision Instruments, Sarasota, FL, USA) were pulled to microelectrodes with a tip diameter of approximately $5 \mu\text{m}$ using a P-2000 micropipette puller (Sutter Instrument, Novato, CA, USA) and silanized with N,N-Dimethyltrimethylsilylamine (Sigma-Aldrich, St. Louis, MO, USA) on a hot plate covered with a glass Petri dish. Silanized microelectrodes were then back-loaded with $100 \text{ mmol l}^{-1} \text{ NH}_4\text{Cl}$ and front-loaded with an approximately $250 \mu\text{m}$ ionophore column of NH_4^+ Ionophore I Cocktail A (Sigma-Aldrich). Probes were calibrated in the same K^+ -free medium containing MS-222 described above to which NH_4Cl was added to final concentrations of 0.1 , 1 , or 10 mmol l^{-1} . pH was maintained at 7.6 across all calibration solutions using NaOH or H_2SO_4 . The slope (in mV) for a tenfold change in NH_4^+ concentration was 59.2 ± 1.1 ($n = 3$).

Larvae were allowed to adjust to the measurement solution for $15\text{--}20 \text{ min}$ prior to flux measurements where thereafter they were restrained in a measurement chamber described previously (Hughes et al., 2019) that prevented larvae from drifting during measurements. NH_4^+ fluxes were measured at the apex of the yolk sac epithelium, similar to previous studies (Shih et al., 2012) and at the pharyngeal region, the latter measurement used as an approximation of gill NH_4^+ flux. Voltage from the NH_4^+ -selective probe was measured approximately $2\text{--}5 \mu\text{m}$ away from the epithelial surface (origin) and at an excursion distance of $100 \mu\text{m}$ away from the epithelium (excursion). Each scan consisted of 5 replicate origin and extrusion measurements and scans were replicated 3 times at the yolk sac and at the jaw for each fish ($n = 1$). For each fish, a background scan was conducted at the beginning and end of the measurement at a location approximately 1 cm away from the larva. Voltage gradients were converted to concentration gradients using the following equation (Donini and O'Donnell, 2005):

$$\Delta C = C_B \times 10^{(\Delta V/S)} - C_B \quad (\text{Eqn 2})$$

where ΔC is the concentration gradient ($\mu\text{mol/cm}^3$) between the origin and excursion points, C_B is the average background ion concentration measured by the probe at all points, ΔV is the

voltage difference (mV) between the origin and excursion points, and S is the slope obtained from the probe calibration (mV). Note that ΔV of the background solution was subtracted from that measured at the epithelium. Flux was then calculated using Fick's law of diffusion:

$$J = D \times \Delta C / \Delta x \quad (\text{Eqn 3})$$

where J is NH_4^+ flux (pmol/cm²/s), D is the diffusion coefficient for NH_4^+ (2.09×10^{-5} cm²/s), and Δx is the excursion distance (cm).

Statistics

All data were tested for normal distribution by Shapiro-Wilk's test. In case data was not normally distributed, data were log transformed. Homogeneity of variances was assessed by Levene's test. If data did not meet the criteria for parametric testing including normal distribution and homogeneity of variances, non-parametric test were applied. Statistical analyses were performed with PAST3 (Hammer et al., 2001). Graphs were generated with GraphPad Prism 9.0 for Windows (GraphPad Software, San Diego, California USA, www.graphpad.com) and Inkscape (<https://inkscape.org>).

Results

Genetic analysis of Hiat1

The three isoforms of DrHiat1 have been referred to as DrHiat1a, DrHiat1b and Hiat1-like according to the current nomenclature used by GenBank. DrHiat1a with 493aa, DrHiat1b with 485aa, and DrHiat1-like with 500aa exhibited a conservation of 323 identical amino acids (ca. 66%), 80 residues as strongly conserved groups (two out of three amino acids identical; ca. 16%), and 19 residues as weakly conserved groups (three different amino acids but with similar properties; ca. 4%). The structure analysis of DrHiat1a, DrHiat1b, and DrHiat1-like by Protter (Omasits et al., 2014) identified 12 predicted transmembrane domains (TM). Furthermore, a sugar binding motif (aa91-108 for DrHiat1a, aa89-106 for DrHiat1b, aa103-120 for Hiat1-like) seems to be associated with TM3 in all three cases. While DrHiat1a and DrHiat1b contained two equivalent phosphoserine/threonine binding groups (aa5-21 / aa5-19, N-terminal; aa299-312 / aa297-310, between TM8 and TM9)(Larner et al., 1993), DrHiat1b contained an additional one between TM1 and TM2 (aa55-70), but DrHiat1-like did not contain any at all. DrHiat1b was the

only isoform to contain a proline-dependent serine/threonine kinase group (Lew et al., 1992; Meyerson et al., 1992)(Cdk5, aa456-469) (Figure S1).

Our preliminary phylogenetic analysis showed Hiat1 to be conserved across many taxa and clustered three distinct clades according to the three different paralogues (Figure 1).

DrHiat1-mediated methylamine (MA) transport in *Xenopus laevis* oocytes

Both DrHiat1a and DrHiat1b-expressing oocytes showed significantly higher (2.7-fold) MA uptake compared to the SHAM (oocytes injected with water, negative control). There was no difference in the uptake of MA between oocytes expressing DrHiat1a or DrHiat1b (Figure 2A; ANOVA with Tukey's pairwise comparisons with $P < 0.001$, $N = 20$).

When exposed to 1 mmol l^{-1} non-labeled NH_4Cl in addition to MA in the medium, the uptake of MA mediated by DrHiat1a and DrHiat1b was reduced by 45% and 40%, respectively. The degree of inhibition of MA by NH_4Cl was not significantly different between oocytes expressing DrHiat1a or DrHiat1b (Figure 2B).

Pre-loaded DrHiat1a- and DrHiat1b-expressing oocytes released significantly more ammonia compared to SHAM-injected oocytes (27% vs. 15%, Figure 3). There was no difference between the amounts of MA released in oocytes expressing Hiat1a compared to Hiat1b.

***In situ* hybridization of Hiat1 isoforms in zebrafish embryos and larvae**

To determine Hiat1 expression in zebrafish, DrHiat1a and DrHiat1b antisense-RNA probes were generated and whole mount *in situ* hybridizations (WISH) was performed on zebrafish embryos and larvae of different developmental stages, beginning from the 4-cell stage until 4 days post-fertilization (dpf) (Figure 4). Maternal expression of both, DrHiat1a (Figure 4A-A) and DrHiat1b (Figure 4B-A) was observed, early onset of transcription during maternal-to-zygotic transition (Figure 4A-B and Figure 4B-B) and ubiquitous expression in all tissues during early segmentation stages (Figure 4A-C and C'; Figure 4B-C and C'). At 24 hours post-fertilization (hpf), towards the end of the segmentation period, expression of both genes is mainly localized to the head region, especially to the fore-, mid- and hindbrain including the midbrain-hindbrain-boundary, the lens and the trigeminal ganglion (Figure 4A-D, D' and figure 4B-D, D'). In addition, DrHiat1a shows distinct expression in the olfactory placode and the hatching gland in

both examined segmentation stages (Figure 4A- C-D'), while DrHiat1b shows additional expression in the optic vesicle, posterior lateral line ganglion and pectoral fin bud at 24 hpf (see Supplementary Figure 1). From 2 dpf to 4 dpf DrHiat1a and DrHiat1b expression can be detected in the brain, heart, gills, digestive system, pectoral fins and parts of the sensory nervous system including cranial and lateral line ganglia (DrHiat1a and DrHiat1b) and the retinal ganglion cell layer and lateral line neuromasts (DrHiat1b) (Figure 4A: E-F'; Figure 4B: E-F' and Supplementary Figure 1). For the digestive system, DrHiat1a appears to be more strongly expressed in the pancreas, whereas DrHiat1b is more present in the intestine (Supplementary Figure 1, E-H). Due to the proteinase K treatment, which was performed from 2 dpf onwards, staining of some of the more external structures, like pectoral fins or lateral line neuromasts, was reduced or even completely abolished. For images without proteinase K treatment see Figure S1.

Ammonia excretion in zebrafish larvae with DrHiat1 knockdown

Successful knockdown of Hiata1a and Hiata1b using splice-blocking morpholinos was verified by PCR where reduced sizes of amplicons (from 450bp to 300bp) indicate successful splice blocking of the 4th exon in pre-mRNA DrHiat1a and DrHiat1b such that the respective exon was not included in mature mRNA (Figure 5A).

Significant reduction of ammonia excretion was found in larvae with DrHiat1b knockdown, but not with DrHiat1a knockdown (Figure 5B). SIET was then used to measure the regional flux of NH_4^+ on larvae with DrHiat1b knockdown (Figure 6A). NH_4^+ selective electrodes were placed at the yolk sac and pharyngeal region (PR)/immature gill regions (Figure 6A). Significant reduction of NH_4^+ flux was detected at both regions in DrHiat1b knockdown larvae compared to the SHAM (Figure 6B).

Discussion

Despite their high level of sequence conservation (86%), hippocampus abundant transporters 1a, 1b and 1-like (Hiata1a, Hiata1b, Hiata1-like; renamed mfsd14a/b in mammals, (Doran et al., 2016; Lekholm et al., 2017) can be clearly distinguished in the phylogenetic analysis. Unfortunately, likely due to the high level of amino acid similarity and the lack of research on the

phylogeny and function of this/these transporter(s), there is currently no consistent nomenclature available in the literature and databases. Consequently, the reader needs to be aware that many proteins annotated as one or the other in the NCBI database did not hold true in our analysis (i.e., many transcripts annotated as Hiat1-like rather cluster as Hiat1b or -1a). It should also be noted that some sequences that were annotated as different isoforms turned out to be simply truncated/not properly assembled versions of the same gene. We therefore present here a potential reference for future annotations of this transporter based on the zebrafish names for each of the Hiat1 paralogues.

Up to date only one isoform of Hiat1 has been identified in invertebrates (Fehsenfeld et al., 2022, under review). Interestingly, while all three isoforms can be identified in teleosts, other vertebrates seem to lack one or more: for lamprey only Hiat1b could be identified, Hiat1-like was not found for elasmobranchs, and no Hiat1a was identified for terrestrial reptilians as well as terrestrial and aquatic mammals. At this point, further phylogenetic analysis would be needed to clarify the exact evolutionary history of the different isoforms.

Zebrafish Hiat1a and Hiat1b as novel ammonia transporters

The present study revealed that both DrHiat1a and DrHiat1b could promote MA uptake when expressed in frog oocytes. Furthermore, MA release was enhanced in pre-loaded oocytes when expressing either of the Hiat1 paralogues. Adding the fact that external ammonia was able to inhibit MA uptake in transgenic oocytes (as seen by the immediate inhibition of MA uptake in the presence of NH_4Cl in the medium) allows us to conclude that also DrHiat1a and DrHiat1b function as ammonia transporters. An equivalent observation was made in the recent study by Fehsenfeld and colleagues in green crabs, where CmHiat1 promoted ammonium transport (likely NH_4^+), shown either directly with scanning ion-selective microelectrodes, or indirectly with radiolabelled MA as a proxy. Despite possessing a sugar transporter-specific motif D-R/K-X-G-R-R/K between TMD2 and TMD3 (Matsuo et al., 1997), recent results clearly showed a lack of glucose transport in *Xenopus laevis* oocytes when expressing crustacean Hiat1 (Fehsenfeld et al., 2022, under review). Similarly, mammalian Mfsd14a was not capable of mediating glucose uptake into the oocyte (Zhouyao et al., 2022).

Interestingly, it should be noted that competition of NH_4^+ transport with MA uptake was only observed in transgenic, but barely in sham-injected oocytes. This might simply be based on the respective concentration of NH_4^+ (1 mmol L^{-1}): a competition might occur at higher

concentrations of NH_4^+ as the kinetics of ammonia/MA transport by endogenous pathways in *Xenopus* oocytes may just have a much higher inhibition constant. Or, in other words, MA uptake by DrHiat1 may have a lower inhibition constant than the endogenous pathways for ammonia uptake of the *Xenopus* oocytes (i.e., via Rhesus-glycoproteins and/or NHE3), such that we see this large difference at $1 \text{ mmol L}^{-1} \text{ NH}_4\text{Cl}$.

Hiat1b-mediated ammonia excretion in zebrafish larvae

Ammonia handling and excretion seem to be especially important in early life stages of fish for a variety of reasons. First, due to an amino acid-focussed metabolism, the ammonia load in fish embryos is substantial (Zimmer et al., 2017). Second, embryos experience physiological constraints; these include the presence of a chorion capsule as a barrier that impedes diffusion between the embryo and its external environment, and the lack of fully functional gills which function as the main ammonia excretory organ in more mature fish (Zimmer et al., 2017).

Generally, ammonia excretion in larval zebrafish occurs in part via H^+ -ATPase-rich (HR) cells in the yolk sac and gills that also contain apical Rhesus-glycoprotein 1 (Rhcg1 or Rhcgb) (Nakada et al., 2007), Na^+/H^+ -exchanger 3 (Ito et al., 2013) and H^+ -ATPase (Lin et al., 2006). Furthermore, with their unique expression patterns along the skin, gills, and yolk sac, Rhag, Rhbg, Rhcg1 (Rhcgb) and Rhcg2 (Rhcg11) have all been shown to contribute to whole zebrafish larvae ammonia excretion to varying extents (Braun et al., 2009; Zimmer and Perry, 2020). Additionally, Rhbg and/or Rhcg1 (Rhcgb) seem to more specifically participate also in the excretion of ammonia via skin keratinocytes (Shih et al., 2008; Shih et al., 2013). In contrast, a $\text{Na}^+/\text{NH}_4^+$ exchange metabolon as mentioned in the introduction, seems to rather contribute to ammonia excretion only under challenging conditions (i.e., low pH and/or low Na^+ environments) and less when fish were kept in unaltered laboratory conditions (i.e., circumneutral water with adequate salt concentrations) (Kumai and Perry, 2011; Shih et al., 2012).

Here, we provide first evidence that ammonia excretion in this early life stage appears to be additionally mediated by DrHiat1b and hence provides an alternative route for basic ammonia transport. Interestingly, Hiat1 is already expressed in frog oocytes and hence maternally provided (Fehsenfeld et al., 2022 under review) so it is ensured to be passed on with the maternal lineage, implying a crucial role for this transporter as early as development begins. The fact that both DrHiat1a and DrHita1b are ubiquitously expressed in the zebrafish embryo and early larvae emphasizes their importance as potential ammonia transporters in this crucial

phase of life. They might provide a very general route for baseline ammonia excretion in every tissue, complemented by more differentially expressed and tissue-specific Rhesus-glycoproteins. It is not surprising that both Hiat1-transcripts can initially be found in the nervous system, resembling the first discovery of Hiat in marsupials' hippocampus (Matsuo et al., 1997). DrHiat1b being more abundantly expressed might indicate its more important role for basic ammonia maintenance and might also explain the subtle differences in tissue expression. For instance, while mRNA for DrHiat1b was present in the intestine, mRNA for DrHiat1a was not detectable.

In DrHiat1b morpholino knock-downs, whole larval ammonia excretion was reduced by ca. 30%. The fact that we observed even further reduction of ammonia excretion when we specifically screened the yolk sac (-75%) and pharyngeal region (immature gill; -85%) underlines the complexity of excretory mechanisms in this stage. Similar discrepancies have been observed in earlier studies on zebrafish larvae, when for example, Zimmer and Perry (2020) found that a knock-down of Rhcgb resulted in an increase of whole larvae ammonia excretion, whereas NH_4^+ flux at the yolk sac assessed by SIET was reduced in response to knockdown using the same morpholino (Shih et al., 2008, 2012). Further thorough investigations are needed to fully understand these respective mechanisms, including potential off-target effects and/or compensatory responses caused by the knock-down, i.e., the possibility that other ammonia transporters like Rhesus-glycoproteins take over for the loss of Hiat1 (Kok et al., 2015; Rossi et al., 2015).

Conclusion

The findings of the present study warrant a reconsideration of ammonia-related transport processes in the gills and potentially other excretory organs of fish. We show here that especially early on in development, the involvement of Hiat1b and/or Hiat1a provides an alternate route for ammonia transport besides the involvement of Rhesus-glycoproteins and/or $\text{Na}^+/\text{NH}_4^+$ exchange metabolon. Alternatively, Hiat1a/1b could be part of the latter. It would be highly desirable for future studies to identify the transporters' exact cellular localization in the branchial membrane to allow for more detailed modelling of branchial ammonia transport. Clearly, Hiat1 transporters have to be taken into account in future studies on ammonia transport in fish and other species, including the mammalian kidney.

Acknowledgements

We like to thank the Animal Care and Veterinary Services at the University of Ottawa, and in particular Christine Archer and Vishal Saxena for taking care of the zebrafish.

Competing interests

The authors declare no competing interests.

Funding

Financial support was provided by Natural Sciences and Engineering Research Council of Canada Discovery grants (NSERC RGPIN-5013-2018 to Dirk Weihrauch, RGPIN-2018-06027 to Peter Eck, and NSERC # G13017 to Steve Perry). The research was further supported by a University of Manitoba UCRP grant (2017-18/SUB 318995) to Dirk Weihrauch and Peter Eck. Haonan Zhouyao was awarded a Company of Biologists travel grant for this collaboration. Sandra Fehsenfeld and Alex Zimmer are/were the recipients of a NSERC postdoctoral fellowship.

References

- Adlimoghaddam, A., Boeckstaens, M., Marini, A. M., Treberg, J. R., Brassinga, A. K. C., & Weihrauch, D. (2015). Ammonia excretion in *Caenorhabditis elegans*: Mechanism and evidence of ammonia transport of the Rhesus protein CeRhr-1. *Journal of Experimental Biology*, 218(5), 675–683. <https://doi.org/10.1242/jeb.111856>
- Adlimoghaddam, A., O'Donnell, M. J., Kormish, J., Banh, S., Treberg, J. R., Merz, D., & Weihrauch, D. (2016). Ammonia excretion in *Caenorhabditis elegans*: Physiological and molecular characterization of the rhr-2 knock-out mutant. *Comparative Biochemistry and Physiology -Part A : Molecular and Integrative Physiology*, 195(April), 46–54. <https://doi.org/10.1016/j.cbpa.2016.02.003>
- Altschul, S. F., Madden, T. L., Schaffer, A. A., Zhang, J., Zhang, Z., Miller, W., & Lipman, D. J. (1997). Gapped BLAST and PSI-BLAST: a new generation of protein database search programs. *Nucleic Acids Research*, 25(17), 3389–3402. [https://doi.org/10.1016/0031-9422\(92\)80418-E](https://doi.org/10.1016/0031-9422(92)80418-E)

- Arillo, A., Margiocco, C., Melodia, F., Mesi, P., & Schenone, G. (1981). Ammonia toxicity mechanism in fish: Studies on rainbow trout (*Salmo gairdneri* Rich.). *Ecotoxicology and Environmental Safety*, 5(3), 316–328. <https://doi.org/10.1016/j.ecoenv.2005.12.006>
- Boo, M. V., Hiong, K. C., Goh, E. J. K., Choo, C. Y. L., Wong, W. P., Chew, S. F., & Ip, Y. K. (2018). The ctenidium of the giant clam, *Tridacna squamosa*, expresses an ammonium transporter 1 that displays light-suppressed gene and protein expression and may be involved in ammonia excretion. *Journal of Comparative Physiology B: Biochemical, Systemic, and Environmental Physiology*, 188(5), 765–777. <https://doi.org/10.1007/s00360-018-1161-6>
- Braun, M. H., Steele, S. L., Ekker, M., & Perry, S. F. (2009). Nitrogen excretion in developing zebrafish (*Danio rerio*): A role for Rh proteins and urea transporters. *American Journal of Physiology - Renal Physiology*, 296(5), F994–F1005. <https://doi.org/10.1152/ajprenal.90656.2008>
- Bucking, C. (2017). A broader look at ammonia production, excretion, and transport in fish: a review of impacts of feeding and the environment. *Journal of Comparative Physiology B*, 187(1), 1–18. <https://doi.org/10.1007/s00360-016-1026-9>
- Cameron, J. N., & Heisler, N. (1983). Studies of ammonia in the rainbow trout: physico-chemical parameters, acid-base behaviour and respiratory clearance. *Journal of Experimental Biology*, 105(1), 107–125. Retrieved from <http://jeb.biologists.org/content/105/1/107.short>
- Chasiotis, H., Ionescu, A., Misyura, L., Bui, P., Fazio, K., Wang, J., ... Donini, A. (2016). An animal homolog of plant Mep/Amt transporters promotes ammonia excretion by the anal papillae of the disease vector mosquito *Aedes aegypti*. *Journal of Experimental Biology*, 219(9), 1346–1355. <https://doi.org/10.1242/jeb.134494>
- Diricx, M., Sinha, A. K., Liew, H. J., Mauro, N., Blust, R., & De Boeck, G. (2013). Compensatory responses in common carp (*Cyprinus carpio*) under ammonia exposure: Additional effects of feeding and exercise. *Aquatic Toxicology*, 142–143, 123–137. <https://doi.org/10.1016/j.aquatox.2013.08.007>
- Donini, A., & O'Donnell, M. J. (2005). Analysis of Na⁺, Cl⁻, K⁺, H⁺ and NH₄⁺ concentration gradients adjacent to the surface of anal papillae of the mosquito *Aedes aegypti*: application of self-referencing ion-selective microelectrodes. *Journal of Experimental Biology*, 208, 603–610. <https://doi.org/10.1242/jeb.01422>
- Doran, J., Walters, C., Kyle, V., Wooding, P., Hammett-burke, R., & Colledge, W. H. (2016). *Mfsd14a* (*Hiat1*) gene disruption causes globozoospermia and infertility in male mice. *Reproduction*, 152, 91–99. <https://doi.org/10.1530/REP-15-0557>
- Dosdat, A., Ruyet, J. P.-L., Coves, D., Dutto, G., Gasset, E., Le Roux, A., & Lemarie, G. (2003). Effect of chronic exposure to ammonia on growth, food utilisation and metabolism of the European sea bass (*Dicentrarchus labrax*). *Aquatic Living Resources*, 16(6), 509–520.
- Durant, A. C., & Donini, A. (2018). Ammonia excretion in an osmoregulatory syncytium is facilitated by AeAmt2, a novel ammonia transporter in *Aedes aegypti* larvae. *Frontiers in Physiology*, 9, 1–16. <https://doi.org/10.3389/fphys.2018.00339>

- Edgar, R. C. (2004). MUSCLE: a multiple sequence alignment method with reduced time and space complexity. *BMC Bioinformatics*, 5, 113.
- Fehsenfeld, S., Kiko, R., Appelhans, Y. S., Towle, D. W., Zimmer, M., & Melzner, F. (2011). Effects of elevated seawater $p\text{CO}_2$ on gene expression patterns in the gills of the green crab, *Carcinus maenas*. *BMC Genomics*, 12(1), 488. <https://doi.org/10.1186/1471-2164-12-488>
- Fehsenfeld, S., Quijada-Rodriguez, A. R., Zhouyao, H., Durant, A. C., Donini, A., Sachs, M., ... Weihrauch, D. (2022). HIAT1 – a new highly conserved transporter involved in ammonia regulation. *FASEB Journal*, (under review).
- Fehsenfeld, S., & Wood, C. M. (2018). Section-specific expression of acid-base and ammonia transporters in the kidney tubules of the goldfish *Carassius auratus* and their responses to feeding. *American Journal of Physiology - Renal Physiology*, 315(6), F1565–F1582. <https://doi.org/10.1152/ajprenal.00510.2017>
- Hammer, Ø., Harper, D. A. T., & Ryan, P. D. (2001). PAST: Paleontological statistics software package for education and data analysis. *Palaeontologia Electronica*, 4(1), 1–9. <https://doi.org/10.1016/j.bcp.2008.05.025>
- Hans, S., Quijada-Rodriguez, A. R., Allen, G. J. P., Onken, H., Treberg, J. R., & Weihrauch, D. (2018). Ammonia excretion and acid-base regulation in the American horseshoe crab, *Limulus polyphemus*. *Journal of Experimental Biology*, 221, jeb151894. <https://doi.org/10.1242/jeb.151894>
- Hughes, M. C., Zimmer, A. M., & Perry, S. F. (2019). Role of internal convection in respiratory gas transfer and aerobic metabolism in larval zebrafish (*Danio rerio*). *American Journal of Physiology - Regulatory Integrative and Comparative Physiology*, 316(3), R255–R264. <https://doi.org/10.1152/ajpregu.00315.2018>
- Ito, Y., Kobayashi, S., Nakamura, N., Miyagi, H., Esaki, M., Hoshijima, K., & Hirose, S. (2013). Close association of carbonic anhydrase (CA2a and CA15a), Na^+/H^+ exchanger (Nhe3b), and ammonia transporter Rhcg1 in zebrafish ionocytes responsible for Na^+ uptake. *Frontiers in Physiology*, 4, 1–17. <https://doi.org/10.3389/fphys.2013.00059>
- Jones, D. T., Taylor, W. R., & Thornton, J. M. (1992). The rapid generation of mutation data matrices from protein sequences. *Computer Applications in the Biosciences*, 8(3), 275–282.
- Kok, F. O., Shin, M., Ni, C. W., Gupta, A., Grosse, A. S., VanImpel, A., ... Lawson, N. D. (2015). Reverse genetic screening reveals poor correlation between morpholino-induced and mutant phenotypes in zebrafish. *Developmental Cell*, 32, 97–108. <https://doi.org/10.1016/j.devcel.2014.11.018>
- Kumai, Y., & Perry, S. F. (2011). Ammonia excretion via Rhcg1 facilitates Na^+ uptake in larval zebrafish, *Danio rerio*, in acidic water. *American Journal of Physiology - Regulatory Integrative and Comparative Physiology*, 301(5), R1517–R1528. <https://doi.org/10.1152/ajpregu.00282.2011>
- Kumar, S., Stecher, G., Li, M., Knyaz, C., & Tamura, K. (2018). MEGA X: Molecular evolutionary genetics analysis across computing platforms. *Molecular Biology and Evolution*, 35(6), 1547–1549. <https://doi.org/10.1093/molbev/msy096>

- Larner, A. C., David, M., Feldman, G. M., Igarashi, K. I., Hackett, R. H., Webb, D. S. A., ... Finbloom, D. S. (1993). Tyrosine phosphorylation of DNA binding proteins by multiple cytokines. *Science*, 261(5129), 1730–1733. <https://doi.org/10.1126/science.8378773>
- Larsen, E. H., Deaton, L. E., Onken, H., O'Donnell, M., Grosell, M., Dantzler, W. H., & Weihrauch, D. (2014). Osmoregulation and excretion. *Comprehensive Physiology*, 4(2), 405–573. <https://doi.org/10.1002/cphy.c130004>
- Lekholm, E., Perland, E., Eriksson, M. M., Hellsten, S. V., Lindberg, F. A., Rostami, J., & Fredriksson, R. (2017). Putative membrane-bound transporters MFSD14A and MFSD14B are neuronal and affected by nutrient availability. *Frontiers in Molecular Neuroscience*, 10, 1–13. <https://doi.org/10.3389/fnmol.2017.00011>
- Lew, J., Beaudette, K., Litwin, C. M. E., & Wang, J. H. (1992). Purification and characterization of a novel proline-directed protein kinase from bovine brain. *Journal of Biological Chemistry*, 267(19), 13383–13390. [https://doi.org/10.1016/s0021-9258\(18\)42222-3](https://doi.org/10.1016/s0021-9258(18)42222-3)
- Lin, L. Y., Horng, J. L., Kunkel, J. G., & Hwang, P. P. (2006). Proton pump-rich cell secretes acid in skin of zebrafish larvae. *American Journal of Physiology - Cell Physiology*, 290(2), 371–378. <https://doi.org/10.1152/ajpcell.00281.2005>
- Mallery, C. H. (1983). A carrier enzyme basis for ammonium excretion in teleost gill. NH_4^+ -stimulated Na-dependent ATPase activity in *Opsanus beta*. *Comparative Biochemistry and Physiology -- Part A: Physiology*, 74(4), 889–897. [https://doi.org/10.1016/0300-9629\(83\)90364-X](https://doi.org/10.1016/0300-9629(83)90364-X)
- Masui, D. C., Furriel, R. P. M., McNamara, J. C., Mantelatto, F. L. M., & Leone, F. A. (2002). Modulation by ammonium ions of gill microsomal (Na^+ , K^+)-ATPase in the swimming crab *Callinectes danae*: A possible mechanism for regulation of ammonia excretion. *Comparative Biochemistry and Physiology - C Toxicology and Pharmacology*, 132(4), 471–482. [https://doi.org/10.1016/S1532-0456\(02\)00110-2](https://doi.org/10.1016/S1532-0456(02)00110-2)
- Matsuo, N., Kawamoto, S., Matsubara, K., & Okubo, K. (1997). Cloning of a cDNA encoding a novel sugar transporter expressed in the neonatal mouse hippocampus. *Biochemical and Biophysical Research Communications*, 238, 126–129. <https://doi.org/10.1006/bbrc.1997.7252>
- Mckenzie, D. J., Shingles, A., Claireaux, G., & Domenici, P. (2009). Sublethal concentrations of ammonia impair performance of the teleost fast-start escape response. *Physiological and Biochemical Zoology*, 82(4), 353–362. <https://doi.org/10.1086/590218>
- McKenzie, D. J., Shingles, A., & Taylor, E. W. (2003). Sub-lethal plasma ammonia accumulation and the exercise performance of salmonids. *Comparative Biochemistry and Physiology - A Molecular and Integrative Physiology*, 135(4), 515–526. [https://doi.org/10.1016/S1095-6433\(03\)00116-8](https://doi.org/10.1016/S1095-6433(03)00116-8)
- Meyerson, M., Enders, G. H., Wu, C.-L., Su, L.-K., Gorka, C., Nelson, C., ... Tsai, L.-H. (1992). A family of human cdc2-related protein kinases. *EMBO Journal*, 11(8), 2909–2917. <https://doi.org/10.1002/j.1460-2075.1992.tb05360.x>

- Nakada, T., Hoshijima, K., Esaki, M., Nagayoshi, S., Kawakami, K., & Hirose, S. (2007). Localization of ammonia transporter Rhcg1 in mitochondrion-rich cells of yolk sac, gill, and kidney of zebrafish and its ionic strength-dependent expression. *American Journal of Physiology - Regulatory Integrative & Comparative Physiology*, (293), R1743–R1753. <https://doi.org/10.1152/ajpregu.00248.2007>.
- Nawata, C. M., Hirose, S., Nakada, T., Wood, C. M., & Kato, A. (2010). Rh glycoprotein expression is modulated in pufferfish (*Takifugu rubripes*) during high environmental ammonia exposure. *The Journal of Experimental Biology*, 213, 3150–3160. <https://doi.org/10.1242/jeb.044719>
- Obenauer, J. C., Cantley, L. C., & Yaffe, M. B. (2003). Scansite 2.0: Proteome-wide prediction of cell signalling interactions using short sequence motifs. *Nucleic Acids Research*, 31(13), 3635–3641. <https://doi.org/10.1093/nar/gkg584>
- Omasits, U., Ahrens, C. H., Mu, S., & Wollscheid, B. (2014). Sequence analysis Protter: interactive protein feature visualization and integration with experimental proteomic data. *Bioinformatics*, 30(6), 884–886. <https://doi.org/10.1093/bioinformatics/btt607>
- Pitts, R. J., Derryberry, S. L., Poulos, F. E., & Zwiebel, L. J. (2014). Antennal-expressed ammonium transporters in the malaria vector mosquito *Anopheles gambiae*. *PLoS ONE*, 9(10), e111858. <https://doi.org/10.1371/journal.pone.0111858>
- Quijada-Rodriguez, A. R., Schultz, A. G., Wilson, J. M., He, Y., Allen, G. J. P., Goss, G. G., & Weihrauch, D. (2017). Ammonia-independent sodium uptake mediated by Na⁺ channels and NHEs in the freshwater ribbon leech *Nephelopsis obscura*. *Journal of Experimental Biology*, 220(18), 3270–3279. <https://doi.org/10.1242/jeb.159459>
- Rossi, A., Kontarakis, Z., Gerri, C., Nolte, H., Hölper, S., Krüger, M., & Stainier, D. Y. R. (2015). Genetic compensation induced by deleterious mutations but not gene knockdowns. *Nature*, 524, 230–233. <https://doi.org/10.1038/nature14580>
- Sayer, M. D. J., & Davenport, J. (1987). The relative importance of the gills to ammonia and urea excretion in five seawater and one freshwater teleost species. *Journal of Fish Biology*, 31, 561–570. <https://doi.org/10.1111/j.1095-8649.1987.tb05258.x>
- Shih, T. H., Horng, J. L., Hwang, P. P., & Lin, L. Y. (2008). Ammonia excretion by the skin of zebrafish (*Danio rerio*) larvae. *American Journal of Physiology - Cell Physiology*, 295(6), C1625–C1632. <https://doi.org/10.1152/ajpcell.00255.2008>
- Shih, T. H., Horng, J. L., Lai, Y. T., & Lin, L. Y. (2013). Rhcg1 and Rhbg mediate ammonia excretion by ionocytes and keratinocytes in the skin of zebrafish larvae: H⁺-ATPase-linked active ammonia excretion by ionocytes. *American Journal of Physiology - Regulatory Integrative and Comparative Physiology*, 304(12), R1130–R1138. <https://doi.org/10.1152/ajpregu.00550.2012>
- Shih, T. H., Horng, J. L., Liu, S. T., Hwang, P. P., & Lin, L. Y. (2012). Rhcg1 and NHE3b are involved in ammonium-dependent sodium uptake by zebrafish larvae acclimated to low-sodium water. *American Journal of Physiology - Regulatory Integrative and Comparative Physiology*, 302, R84–R93. <https://doi.org/10.1152/ajpregu.00318.2011>

- Shingles, A., McKenzie, D. J., Taylor, E. W., Moretti, A., Butler, P. J., & Ceradini, S. (2001). Effects of sublethal ammonia exposure on swimming performance in rainbow trout (*Oncorhynchus mykiss*). *Journal of Experimental Biology*, 204(15), 2691–2698. <https://doi.org/10.1242/jeb.204.15.2691>
- Sinha, A. K., Liew, H. J., Diricx, M., Blust, R., & De Boeck, G. (2012). The interactive effects of ammonia exposure, nutritional status and exercise on metabolic and physiological responses in gold fish (*Carassius auratus* L.). *Aquatic Toxicology*, 109, 33–46. <https://doi.org/10.1016/j.aquatox.2011.11.002>
- Sinha, A. K., Liew, H. J., Diricx, M., Kumar, V., Darras, V. M., Blust, R., & De Boeck, G. (2012). Combined effects of high environmental ammonia, starvation and exercise on hormonal and ion-regulatory response in goldfish (*Carassius auratus* L.). *Aquatic Toxicology*, 114–115, 153–164. <https://doi.org/10.1016/j.aquatox.2012.02.027>
- Smith, A. A., Zimmer, A. M., & Wood, C. M. (2012). Branchial and extra-branchial ammonia excretion in goldfish (*Carassius auratus*) following thermally induced gill remodeling. *Comparative Biochemistry and Physiology A*, 162, 185–192. <https://doi.org/10.1016/j.cbpa.2012.02.019>
- Smith, H. W. (1929). The excretion of ammonia and urea by the gills of fish. *Journal of Biological Chemistry*, 81(3), 727–742. [https://doi.org/10.1016/s0021-9258\(18\)63725-1](https://doi.org/10.1016/s0021-9258(18)63725-1)
- Thiel, D., Hugenschutt, M., Meyer, H., Paululat, A., Quijada-Rodriguez, A. R., Purschke, G., & Weihrauch, D. (2017). Ammonia excretion in the marine polychaete *Eurythoe complanata* (Annelida). *Journal of Experimental Biology*, 220(3), 425–436. <https://doi.org/10.1242/jeb.145615>
- Thisse, C., & Thisse, B. (2008). High-resolution in situ hybridization to whole-mount zebrafish embryos. *Nature Protocols*, 3(1), 59–69. <https://doi.org/10.1038/nprot.2007.514>
- Verdouw, H., Van Echteld, C. J. A., & Dekkers, E. M. J. (1978). Ammonia determination based on indophenol formation with sodium salicylate. *Water Research*, 12, 399–402. [https://doi.org/10.1016/0043-1354\(78\)90107-0](https://doi.org/10.1016/0043-1354(78)90107-0)
- Wall, S. M., & Koger, L. M. (1994). NH_4^+ transport mediated by Na^+-K^+ -ATPase in rat inner medullary collecting duct. *American Journal of Physiology - Renal Physiology*, 267(4 Pt 2), F660–F670. <https://doi.org/10.1152/ajprenal.1994.267.4.f660>
- Weihrauch, D., Chan, A. C., Meyer, H., Döring, C., Sourial, M., & O'Donnel, M. J. (2012). Ammonia excretion in the freshwater planarian *Schmidtea mediterranea*. *Journal of Experimental Biology*, 215(18), 3242–3253. <https://doi.org/10.1242/jeb.067942>
- White, R. M., Sessa, A., Burke, C., Bowman, T., LeBlanc, J., Ceol, C., ... Zon, L. I. (2008). Transparent adult zebrafish as a tool for in vivo transplantation analysis. *Cell Stem Cell*, 2(2), 183–189. <https://doi.org/10.1016/j.stem.2007.11.002>
- Wilkie, M. P. (1997). Mechanisms of ammonia excretion across fish gills. *Comparative Biochemistry and Physiology - A Physiology*, 118A(1), 39–50. [https://doi.org/10.1016/S0300-9629\(96\)00407-0](https://doi.org/10.1016/S0300-9629(96)00407-0)

- Wood, C. M., & Nawata, C. M. (2011). A nose-to-nose comparison of the physiological and molecular responses of rainbow trout to high environmental ammonia in seawater versus freshwater. *Journal of Experimental Biology*, 214(21), 3557–3569. <https://doi.org/10.1242/jeb.057802>
- Wright, P. A., & Wood, C. M. (2009). A new paradigm for ammonia excretion in aquatic animals: role of Rhesus (Rh) glycoproteins. *The Journal of Experimental Biology*, 212, 2303–2312. <https://doi.org/10.1242/jeb.023085>
- Zhouyao, H., Fehsenfeld, S., Weihrauch, D., & Eck, K. P. (2022). The murine major facilitator superfamily domain containing 14A (*Mfsd14a*) gene does not encode a glucose transporter. *Advances in Nutrition and Food Science*, 2022(02), 1–13. <https://doi.org/10.37722/ANAFS.2022101>
- Zimmer, A. M., Brauner, C. J., & Wood, C. M. (2014). Ammonia transport across the skin of adult rainbow trout (*Oncorhynchus mykiss*) exposed to high environmental ammonia (HEA). *Journal of Comparative Physiology B: Biochemical, Systemic, and Environmental Physiology*, 184, 77–90. <https://doi.org/10.1007/s00360-013-0784-x>
- Zimmer, A. M., & Perry, S. F. (2020). The Rhesus glycoprotein Rhcgb is expendable for ammonia excretion and Na⁺ uptake in zebrafish (*Danio rerio*). *Comparative Biochemistry and Physiology -Part A : Molecular and Integrative Physiology*, 247, 110722. <https://doi.org/10.1016/j.cbpa.2020.110722>
- Zimmer, A. M., Wright, P. A., & Wood, C. M. (2017). Ammonia and urea handling by early life stages of fishes. *Journal of Experimental Biology*, 220(21), 3843–3855. <https://doi.org/10.1242/jeb.140210>

Figures

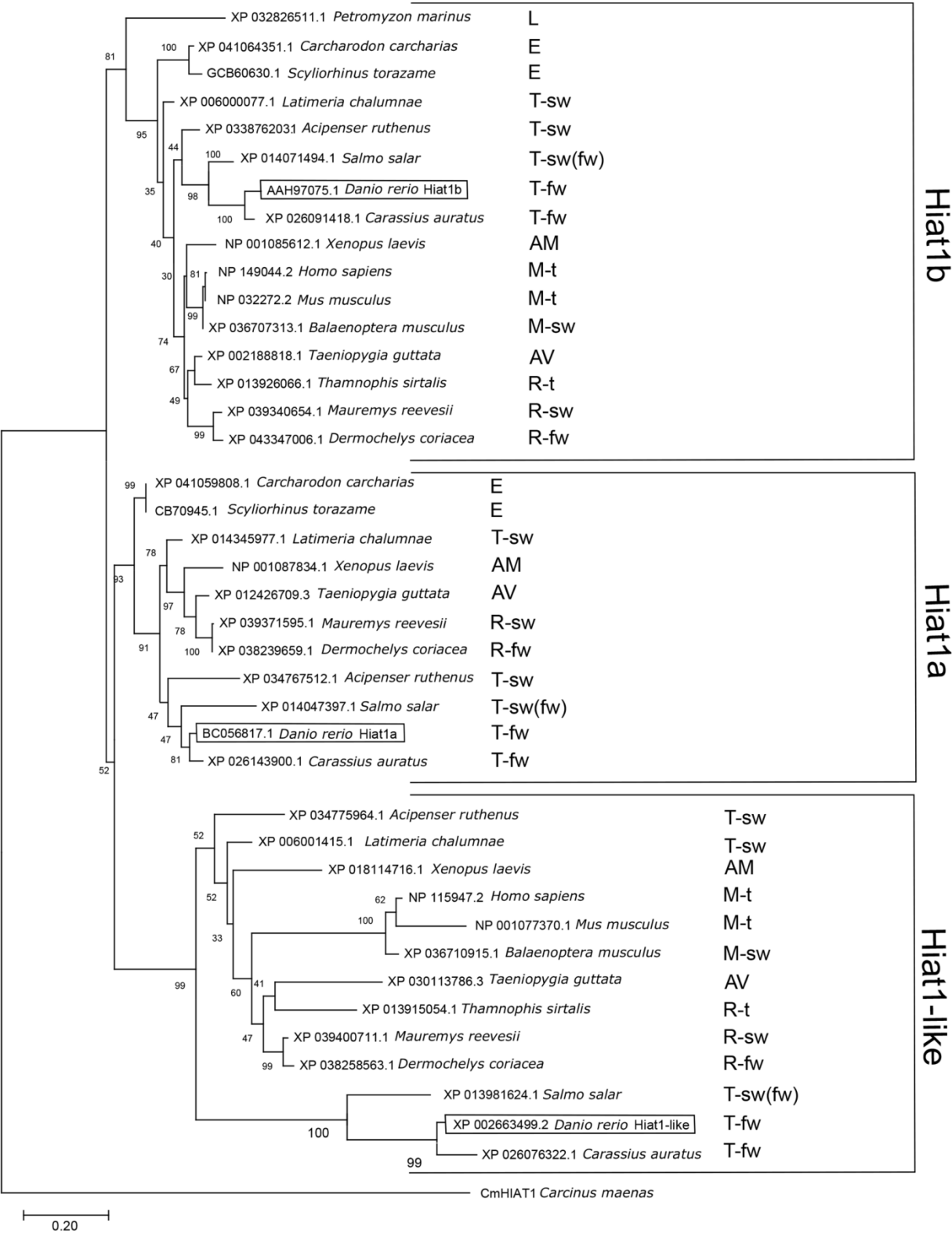


Fig. 1. Phylogenetic analysis of Hiat1-like, Hiat1a and Hiat1b across vertebrates. Shown is the Maximum likelihood consensus tree of the MUSCLE alignment (Edgar, 2004) of Hiat1 proteins as performed with MEGAX (Kumar et al., 2018). Numbers beside branches represent bootstrap values (1000 replicates). The tree is drawn to scale, with branch lengths measured in the number of substitutions per site (indicated by bar at bottom). AM, amphibia; AV, aves; E, elasmobranchii; L, lamprey; M-sw, marine mammalia; M-t, terrestrial mammalia; R-fw, freshwater reptilia; R-sw, seawater reptilia; R-t, terrestrial reptilia, T-fw, freshwater teleostei; T-sw, seawater teleostei. *Salmo salar* has been indicated as both marine and freshwater as it returns to freshwater for reproduction. The tree has been rooted by including the recently identified Hiat-protein in the green crab, *Carcinus maenas* (Fehsenfeld et al., 2022 under review).

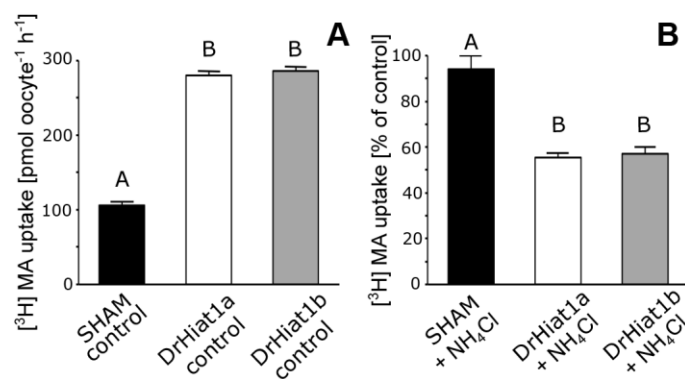


Fig. 2. DrHiat1a and DrHiat1b-mediated methylamine/methylammonium (MA) uptake in *Xenopus laevis* oocytes. (A) Absolute [³H]-methylamine/methylammonium (MA) uptake of sham-injected oocytes (black bar) and oocytes expressing DrHiat1a (white bar) or DrHiat1b (dark grey bar) under control conditions (medium pH 7.2). (B) Relative [³H] MA uptake of sham-injected oocytes (black bar) and oocytes expressing DrHiat1a (white bar) or DrHiat1b (dark grey bar) in medium containing 1 mmol L⁻¹ NH₄Cl. Values in (B) are depicted as % of the corresponding control values as shown in figure 2A. Data are shown as means ± s.e.m. Uppercase letters indicate significant differences as identified with one-way ANOVA and Tukey's post-hoc test ($P < 0.001$, $N = 19,20,20$).

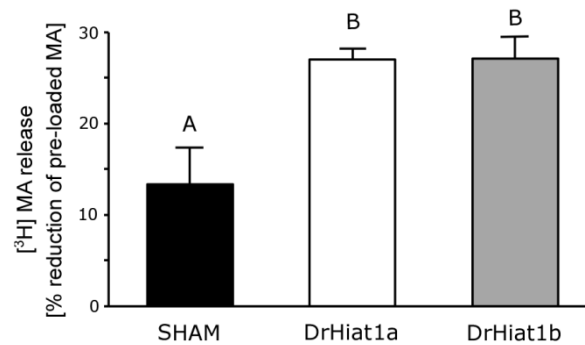
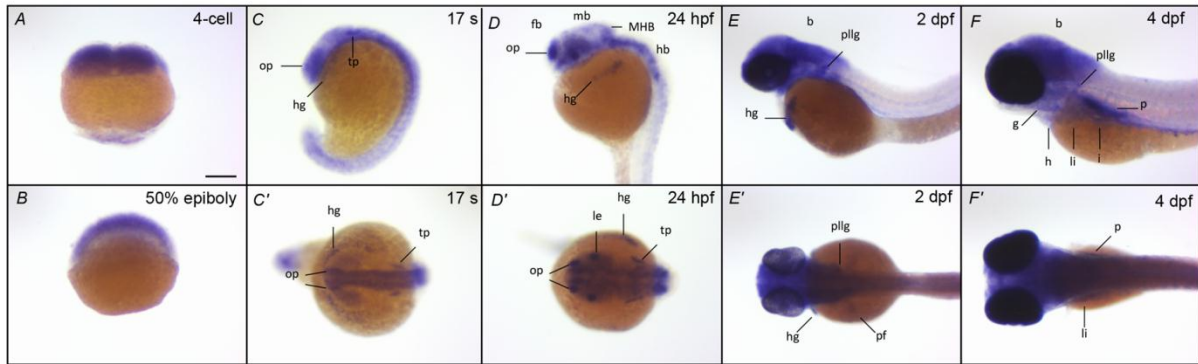


Fig. 3. Relative methylamine/methylammonium (MA) release of pre-loaded *Xenopus laevis* oocytes expressing DrHiat1a or DrHiat1b. Oocytes were pre-loaded in MA-containing medium for 60 min after which internal oocyte MA concentration was measured (MA_{pre}). Subsequently, oocytes were transferred to MA-free medium and re-counted after additional 60 min (MA_{rel}). The graph shows the MA release relative to pre-loaded values calculated as $MA \text{ release} = 100\% - (MA_{rel} / MA_{pre} * 100\%)$. Data are shown as means \pm s.e.m. Uppercase letters indicate significant differences as identified by Kruskal Wallis test with Mann-Whitney pairwise and Bonferroni corrected comparisons ($P < 0.03$, $N = 20,20,20$).

A *DrHiat1a*



B *DrHiat1b*

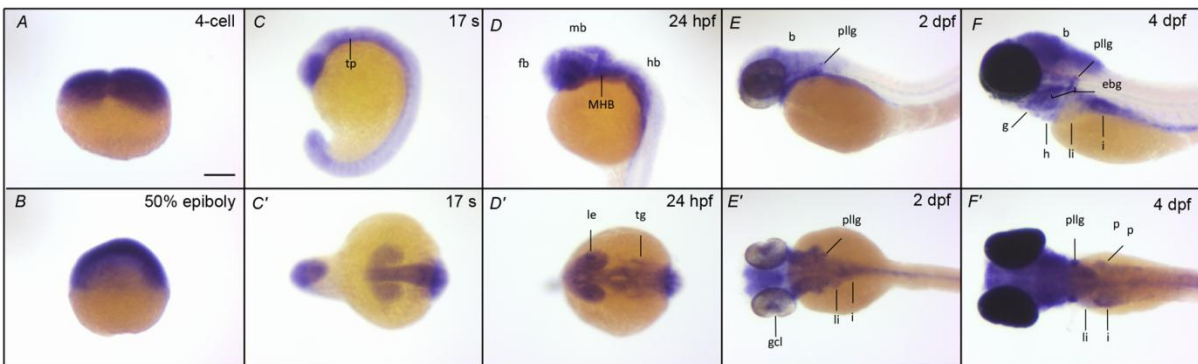


Fig. 4. Expression pattern of *DrHiat1a* and *DrHiat1b* in zebrafish embryos and larvae during early development. Whole mount in situ hybridization of zebrafish, *Danio rerio*, *DrHiat1a* (A) and *DrHiat1b* (B) at the 4-cell stage, 50% maternal-to-zygotic transition (50% epiboly), 17 somite stage (17s), and 24 hours / 2 days / 4 days post-fertilization (24 hpf / 2 dpf / 4 dpf). A, B: lateral view, animal pole to the top. C-F: lateral view, anterior to the left. C'-F': dorsal view, anterior to the left. b: brain; fb: forebrain; g: gills; h: heart; hb: hindbrain; hg: hatching gland; i: intestine; le: lens; li: liver; mb: midbrain; MHB: midbrain-hindbrain-boundary; op: olfactory placode; p: pancreas; pf: pectoral fin; pllg: posterior lateral line ganglion; tg: trigeminal ganglion; tp: trigeminal placode. Scale bar (for all images): 200 μ m.

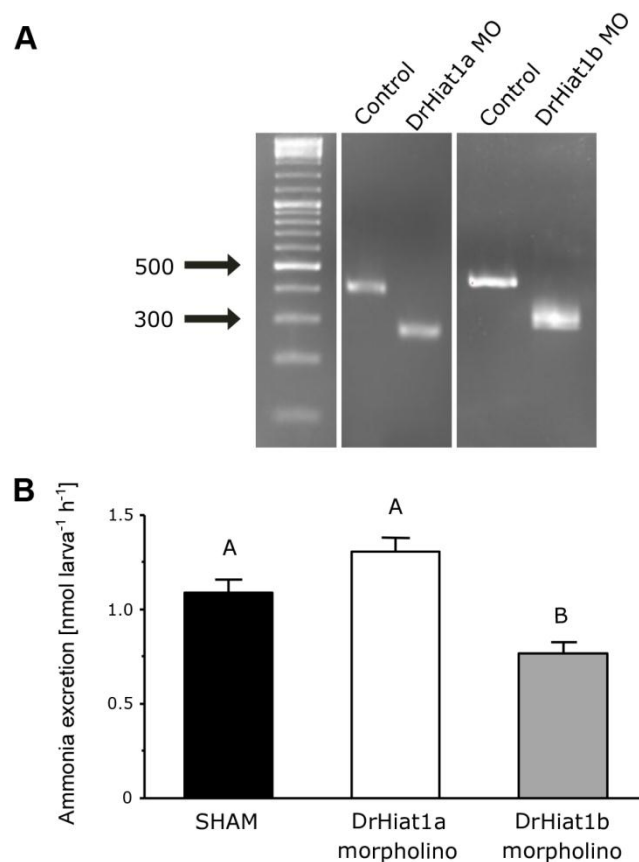


Fig. 5. Whole animal ammonia excretion in DrHiat1a and DrHiat1b knock-down (morpholino) larvae (4dpf). (A) Confirmation of successful DrHiat1a/DrHiat1b knockdown (morpholinos, MO) indicated by a reduced size of PCR products compared to control, caused by blockage of pre-mRNA splicing in the morpholinos. (B) Ammonia excretion in sham-injected larva and DrHiat1a/DrHiat1b knockdown larvae (morpholinos). Data are shown as means \pm s.e.m. Uppercase letters indicate significant differences as identified by Kruskal Wallis test with Mann-Whitney pairwise and Bonferroni corrected comparisons ($P < 0.004$, $N = 41, 24, 29$).

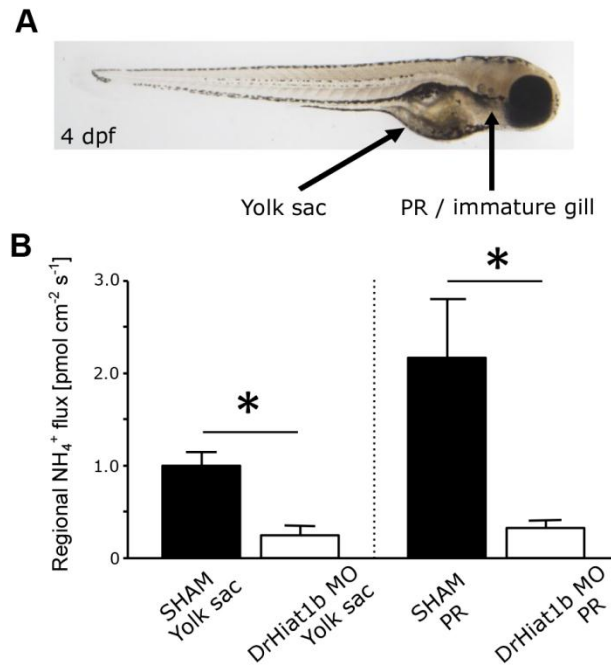


Fig. 6. Regional NH_4^+ flux in DrHiat1b knock-down larvae. (A) Microelectrodes were placed at the yolk sac and pharyngeal region (PR; immature gill) of larvae 4 days post-fertilization (4 dpf). (B) The Scanning Ion-selective micro-Electrode technique (SIET) was used to measure NH_4^+ at these distinct regions in sham and DrHiat1b morpholinos (MO). Data are shown as means \pm s.e.m. Asterisks denote significant differences as identified with Student's t-test ($P < 0.004$, $N = 4-7$ animals per condition and site).

		TM1		
DrHiatla	-----MTGEKKKKRNLNRSILLAKKII IKDGGT PQGIGEPS	VYHAVVVFLEF	48	
DrHiatlb	-----MTQKKKKRVNRSLLLAKKII IKDGGT PQGFGSPS	VYHAVIVIFLEF	46	
DrHiat-like	MRCND EMAMKMMAAQGEKDPKHTRS VLVVKRI IMKHDNPVQQIGKPS	VYHAVVVIFLEF	60	
	* * . : * * . : * * . : * * . : *			
	<u>TM1</u>	<u>TM2</u>	<u>TM3</u>	
DrHiatla	FAWGLLTTPMLAVLRQTFFPQHTFLMNGLIHG VKGLLSFLSAPL	IGALSDVWGGRKS	FLLLT	108
DrHiatlb	FAWGLLTAPFLGALDETFPKHTFLMNGLIQG VKGLLSFLSAPL	IGALS DVWGGRKS	SFLLLT	106
DrHiat-like	FAWGLLTTPMLTVLHETFPHTFLINGLIQG VKGLLSFMSAPL	IGALSDVWGGRS	SFLVLT	120
	***** : * * . : * * : * * : * * : * * : * * : * * : *			
	<u>TM3</u>	<u>TM4</u>	<u>TM5</u>	
DrHiatla	VFFTCAPIPLMKISPPWWYFAVISMSGVF AVTFSVIFAYVADITQEHERST	AYGLVSATFA		168
DrHiatlb	VFFTCAPIPLMKISPPWWYFAMISVSGVF AVTFSVIFAYVADITQEHERSM	AYGMVSATFA		166
DrHiat-like	VFFTCAPIPLMRISPWWYFAMISVSGAFSVTFSVIFAYIADVTDERERST	AYGLVSATFA		180
	***** : * * : * * : * * : * * : * * : * * : * * : * * :			
	<u>TM5</u>	<u>TM6</u>		
DrHiatla	ASLVTSPAIGAYLSSEVYGDTLVVLATAIALLDICFILVAV	PESLP EKM RPASWGAPISW		228
DrHiatlb	ASLVISPAIGAYLSHVYGD TLVVVLASAIA MLDICILVAV	PESLP EKM RPASWGAPISW		226
DrHiat-like	ASLVTSPAIGAYLSASYGNLVVLATIALADICFILLAV	PESLPDKMRLNTWGAPISW		240
	**** ***** ** . * * : * * : * * : * * : * * : * * : *			
	<u>TM7</u>	<u>TM8</u>		
DrHiatla	EQADPFASLRKVGDSTVLLICITVFLSYLPEAGQYSSFFLYLRQVIGFTSET	VAAFI AV		288
DrHiatlb	EQADPFASLRKVGDSTVLLICITVFLSYLPEAGQNSSF LYLQIMGFSSSV	VAAFI AV		286
DrHiat-like	EQADPFASLRKVGDSTVLLICITVFLSYLPEAGQYSSFFLYLRQVINFSPTKI	AVFIGV		300
	***** : * * : * * : * * : * * : * * : * * : * * : * * :			
	<u>TM8</u>	<u>TM9</u>	<u>TM10</u>	
DrHiatla	VGILSILAQT VLVGLLMRSIGNKNTILLGLGFQILQLAWYGFSGQP	WMWAAGAVAAMS		348
DrHiatlb	LGLLSVVAQT VLVSLLMRSIGNKNTILLGLGFQILQLAWYGFSGSEP	WMWAAGAVAAMS		346
DrHiat-like	VGILSILAQTLFLTLLMRTIGNKNTVLLGLGFQILQLAWYGLGSEP	WMWAAGAVAAMS		360
	: * * : * * : * * : * * : * * : * * : * * : * * : * * : * * :			
	<u>TM10</u>	<u>TM11</u>		
DrHiatla	ITFPAISAI VSRNADPDQQGVVGMITGIRGLC NGLGPALYGFVFYL FHV	ELSEMDPAES		408
DrHiatlb	ITFPAVSALT SRADPDQQGVVGMMTGIRGLC NGLGPALYGFIFYIFH	VELDKVP EK-G		405
DrHiat-like	ITFPVASALVSRNADPDQGVGMGTGIRGLC NGLGPALYGFVFLFN	VELSGVETPIQ-		419
	***** : * : * * . * * : * * : * * : * * : * * : * * : * * :			
	<u>TM12</u>			
Hiatla	PEKGVKPNMANPTDES AII PGPFLLFGACSVLLSLLVALFI	PEHNGLNLRPGSYKHHNNG		468
Hiatlb	PDV---QHHRDLHQQS AII PGPFLLFGACSVLLALLVALFI	PEHPHMGTRSGSWKHHTSP		462
Hiat-like	PDFAIP---IQTPTEKT T I PGPFLLGACTV VVAFIVALFI	PDHSTPPSTPCQTR-KNSL		475
	* : : : * * : * * : * * : * * : * * : * * : * * : * * :			
Hiatla	AQSHSSHSSQGGQCEGKEPLEDDSSV		493	
Hiatlb	HG-HPHS-PHPPGEAKEPELLQDTNV		485	
Hiat-like	AGAHTNTPLPGSDEDDFEPLLEDSTV		500	
	* . . . * * * * * . *			

FIG S1

Fig. S1. Alignment of the three *Danio rerio* Hiat1 isoforms. Sequences for DrHiat1-like (GenBank accession number XP_002663499.2), DrHiat1a (GenBank acc. no. BC056817.1) and DrHiat1b (GenBank acc. no. AAH97075.1) were aligned with Clustal Omega (<https://www.ebi.ac.uk/Tools/msa/clustalo/>). Shown are the sugar binding motif in red letters, transmembrane domains in bold and underlined (TMs), Phosphoserine/threonine binding groups in light blue (Neck1) / purple (Neck2) / yellow (Neck6) and a proline-dependent serine/threonine kinase group in green (cyclin-dependent kinase 5 Cdk5). Asterisks denote conserved sites, “.” denote conserved strong groups and “.” denote conservation of weak groups.

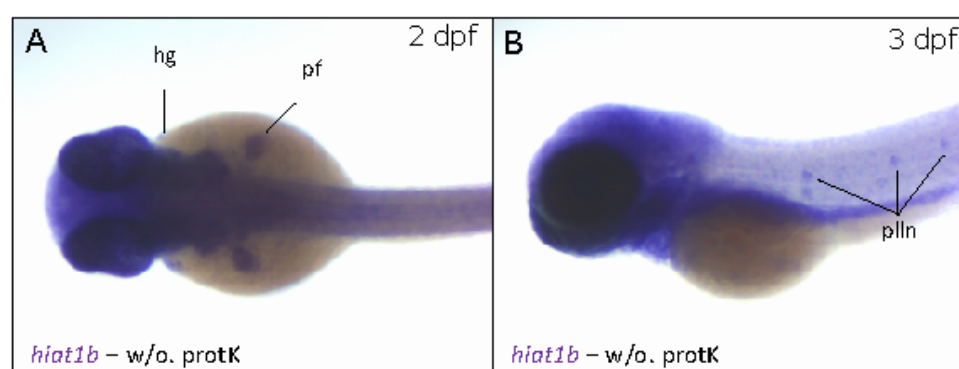


FIG S2

Fig. S2. *In situ* hybridization of DrHiat1b without proteinase K treatment. Additional staining for DrHiat1b can be detected in (B) the pectoral fin (pf) and weakly in the hatching gland (hg) at 2 days post fertilization (dpf), and in (C) the posterior lateral line neuromasts (pll_n) at 3 dpf. B, dorsal view, anterior to the left; C: lateral view, anterior to the left.

Table S1. Protein sequences for phylogenetic tree as shown in figure 1. Accession numbers are according to GenBank.

GenBank accession no.	Clusters as	Species	Common name	Class
NP 001085612.1	Hiat1b	<i>Xenopus laevis</i>	African clawed frog	Amphibia
XP 018114716.1	Hiat1-like	<i>Xenopus laevis</i>	African clawed frog	Amphibia
NP 001087834.1	Hiat1a	<i>Xenopus laevis</i>	African clawed frog	Amphibia
XP 002188818.1	Hiat1b	<i>Taeniopygia guttata</i>	Zebrafinch	Aves
XP 030113786.3	Hiat1-like	<i>Taeniopygia guttata</i>	Zebrafinch	Aves
XP 012426709.3	Hiat1a	<i>Taeniopygia guttata</i>	Zebrafinch	Aves
XP_041064351.1	Hiat1b	<i>Carcharodon carcharias</i>	Great white shark	Chondrichthyes
XP 041059808.1	Hiat1a	<i>Carcharodon carcharias</i>	Great white shark	Chondrichthyes
GCB60630.1	Hiat1b	<i>Scyliorhinus torazame</i>	Cloudy catshark	Chondrichthyes
GCB70945.1	Hiat1a	<i>Scyliorhinus torazame</i>	Cloudy catshark	Chondrichthyes
XP 033876203.1	Hiat1b	<i>Acipenser ruthenus</i>	Sterlet	Chondrostei
XP 034775964.1	Hiat1-like	<i>Acipenser ruthenus</i>	Sterlet	Chondrostei
XP 034767512.1	Hiat1a	<i>Acipenser ruthenus</i>	Sterlet	Chondrostei
DW250260.1	Hiat1	<i>Carcinus maenas</i>	Green crab	Crustacea
XP_032826511.1	Hiat1b	<i>Petromycon marinus</i>	Sea lamprey	Hyperoartia (Agnatha)
NP 149044.2	Hiat1b	<i>Homo sapiens</i>	Human	Mammalia
NP 115947.2	Hiat1-like	<i>Homo sapiens</i>	Human	Mammalia
NP 032272.2	Hiat1b	<i>Mus musculus</i>	House mouse	Mammalia
NP 001077370.1	Hiat1-like	<i>Mus musculus</i>	House mouse	Mammalia
XP 036707313.1	Hiat1b	<i>Balaenoptera musculus</i>	Blue whale	Mammalia (SW)
XP 036710915.1	Hiat1-like	<i>Balaenoptera musculus</i>	Blue whale	Mammalia (SW)
XP 039340654.1	Hiat1b	<i>Mauremys reevesii</i>	Chinese pond turtle	Reptilia (FW)
XP 039400711.1	Hiat1-like	<i>Mauremys reevesii</i>	Chinese pond turtle	Reptilia (FW)
XP 039371595.1	Hiat1a	<i>Mauremys reevesii</i>	Chinese pond turtle	Reptilia (FW)
XP 043347006.1	Hiat1b	<i>Dermochelys coriacea</i>	Leatherback sea turtle	Reptilia (SW)
XP 038258563.1	Hiat1-like	<i>Dermochelys coriacea</i>	Leatherback sea turtle	Reptilia (SW)
XP 038239659.1	Hiat1a	<i>Dermochelys coriacea</i>	Leatherback sea turtle	Reptilia (SW)
XP 013926066.1	Hiat1b	<i>Thamnophis sirtalis</i>	Common garter snake	Reptilia (T)
XP 013915054.1	Hiat1-like	<i>Thamnophis sirtalis</i>	Common garter snake	Reptilia (T)
XP 006000077.1	Hiat1b	<i>Latimeria chalumnae</i>	West Indian ocean coelacanth	Sarcopterygii
XP 006001415.1	Hiat1-like	<i>Latimeria chalumnae</i>	West Indian ocean coelacanth	Sarcopterygii
XP 014345977.1	Hiat1a	<i>Latimeria chalumnae</i>	West Indian ocean coelacanth	Sarcopterygii
XP 026091418.1	Hiat1b	<i>Carassius auratus</i>	Goldfish	Teleostei (FW)
XP 026076322.1	Hiat1-like	<i>Carassius auratus</i>	Goldfish	Teleostei (FW)
XP 026143900.1	Hiat1a	<i>Carassius auratus</i>	Goldfish	Teleostei (FW)
AAH97075.1	Hiat1b	<i>Danio rerio</i>	Zebrafish	Teleostei (FW)
XP 002663499.2	Hiat1-like	<i>Danio rerio</i>	Zebrafish	Teleostei (FW)
BC056817.1	Hiat1a	<i>Danio rerio</i>	Zebrafish	Teleostei (FW)
XP 014071494.1	Hiat1b	<i>Salmo salar</i>	Atlantik salmon	Teleostei (SW)
XP 013981624.1	Hiat1-like	<i>Salmo salar</i>	Atlantik salmon	Teleostei (SW)
XP 014047397.1	Hiat1a	<i>Salmo salar</i>	Atlantik salmon	Teleostei (SW)

Table S2. Primer sequences. Primers have been designed based on GenBank accession numbers XP_002663499.2 (DrHiat1-like), AAH97075.1 (DrHiat1a), and BC056817 (DrHiat1b).

Application	Name	Sequence (5'-3')	Amplicon size (bp)	Annealing temperature (°C)
ORF	DrHiat1a ORF forward	ACCATGACTGGAGAGAAAAAGAAGAAA	493	60
	DrHiat1a ORF reverse	TTATACGCTGTCCTCCAGTAA		
	DrHiat1b ORF forward	ACCATGACCCAGAAAAAGAAGAAGCGA	485	62
	DrHiat1b ORF reverse	TCAGACATTAGTGTCTGAAGG		
Oocytes	DrHiat1a Xmal forward	TCCCCCGGGACCATGACTGGAGAGAAAAAGAAGAAAA	513	65
	DrHiat1a XbaI reverse	GCTCTAGATTATACGCTGCTGTCCTCCAGTAAA		
	DrHiat1b Xmal forward	TCCCCCGGGACCATGACCCAGAAAAAGAAGAAGCGAG	505	65
	DrHiat1b XbaI reverse	GCTCTAGATCAGACATTAGTGTCTGTAGAAGG		
<i>In situ</i>	DrHiat1a insitu forward	AAAATCTAGAAACCATGACTGGAGAGAAAAAGAAGAAAA	513	65
	DrHiat1a insitu reverse	TTTTGGGCCCTACGCTGCTGTCCTCCAGTAAAGGC		
	DrHiat1b insitu forward	AAAATCTAGAACCATGACCCAGAAAAAGAAGAAGCGAG	505	65
	DrHiat1b insitu reverse	TTTTGGGCCCGACATTAGTGTCTGTAGAAGGGGC		
Morpholinos	DrHiat1a MO forward	AAAAGAAGAAAAAGCGGCTGAAC	355	57
	DrHiat1a MO reverse	ACAGCAAACACTCCAGACATGG		
	DrHiat1b MO forward	ATTCTGGAGTTCTTCGCTTGG	373	57
	DrHiat1b MO reverse	GACTGAGATACGCACCGATGG		